Characterizing hydrophobicity of amino acid side chains in a protein environment via measuring contact angle of a water nanodroplet on planar peptide network

Chongqin Zhu[a,b,1], Yurui Gao[a,1], Hui Li[c,d,1], Sheng Meng[c,d,e], Lei Li[a], Joseph S. Francisco[a,2], and Xiao Cheng Zeng[a,b,2]

[a]Department of Chemistry, University of Nebraska–Lincoln, Lincoln, NE 68588; [b]Beijing Advanced Innovation Center for Soft Matter Science and Engineering, Beijing University of Chemical Technology, Beijing 100029, China; [c]Beijing National Laboratory for Condensed Matter Physics, Chinese Academy of Sciences, Beijing 100190, China; [d]Institute of Physics, Chinese Academy of Sciences, Beijing 100190, China; and [e]Collaborative Innovation Center of Quantum Matter, Beijing 100190, China

Contributed by Joseph S. Francisco, September 30, 2016 (sent for review September 1, 2016; reviewed by Liem Dang and Wei Yang)

Hydrophobicity of macroscopic planar surface is conventionally characterized by the contact angle of water droplets. However, this engineering measurement cannot be directly extended to surfaces of proteins, due to the nanometer scale of amino acids and inherent nonplanar structures. To measure the hydrophobicity of side chains of proteins quantitatively, numerous parameters were developed to characterize behavior of hydrophobic solvation. However, consistency among these parameters is not always apparent. Herein, we demonstrate an alternative way of characterizing hydrophobicity of amino acid side chains in a protein environment by constructing a monolayer of amino acids (i.e., artificial planar peptide network) according to the primary and the β-sheet secondary structures of protein so that the conventional engineering measurement of the contact angle of a water droplet can be brought to bear. Using molecular dynamics simulations, contact angles θ of a water nanodroplet on the planar peptide network, together with excess chemical potentials of purely repulsive methane-sized Weeks–Chandler–Andersen solute, are computed. All of the 20 types of amino acids and the corresponding planar peptide networks are studied. Expectedly, all of the planar peptide networks with nonpolar amino acids are hydrophobic due to $\theta > 90°$, whereas all of the planar peptide networks of the polar and charged amino acids are hydrophilic due to $\theta < 90°$. Planar peptide networks of the charged amino acids exhibit complete-wetting behavior due to $\theta = 0°$. This computational approach for characterization of hydrophobicity can be extended to artificial planar networks of other soft matter.

hydrophobicity | amino acids | contact angle | nanodroplet | water

Hydrophobic effect on the microscopic level can be understood via analysis of unfavorable ordering of water molecules around nonpolar solutes, where dynamic hydrogen bonds among water molecules nearby can be disrupted (1). The hydrophobic interaction is well known as one of the major driving forces for protein folding, and is also a key factor to stabilize the globular or binding structures of single protein, multiprotein, and protein–ligand systems (2–5). According to previous studies, the hydrophobicity of proteins can be attributed mainly to the side chains of amino acid residues, which are the structural units of protein backbones (5–7). Hence, quantitative characterization of the hydrophobicity of amino acids in protein environment is crucial to our understanding of the protein functionalities in biological environment and also to the prediction of synthetic peptide structures.

Over the past three decades, extensive studies have been devoted to understanding hydrophobic interaction and hydrophobic hydration on the molecular levels (8–37). However, the quantitative description of the hydrophobicity of protein and amino acid residues still largely hinges on molecular thermodynamic properties of the residues rather the structural properties of the protein polymer itself. In engineering fields, the hydrophobicity of a macroscopic planar surface is usually characterized by measuring the contact angle (CA) of water droplets on the surface. This conventional method is not feasible for proteins, however, due to its high curvature and nanoscale size (38–40). Because of this experimental limitation, instead of measuring CA, researchers have developed other indirect methods to characterize relative hydrophobicity of amino acid residues. One of widely used methods is based on a partition of amino acids in two immiscible liquid phases (8–16). Using ethanol and dioxane as the organic solvents to model the protein interior, Nozaki and Tanford (8) proposed a scale for quantitative description of the hydrophobicity of amino acids. It turns out that other phases, such as micellar and vapor phases, can be also coupled with the partition method to avoid possible inaccurate account of cavity formation energy in organic solvents (41, 42). Radzicka and Wolfenden (13) analyzed vapor–liquid free energy data and identified a correlation between hydration potential of amino acid and its accessible surface area in known protein structures. Baldwin (43) found that the hydrophobic free energy computed based on the vapor–liquid transfer is significantly reduced, but is still a dominant factor in protein folding. One issue with the partitioning method is that neither the organic solvent nor the vapor phase can precisely mimic the protein interior that

Significance

Quantitative characterization of hydrophobicity of amino acid side chains in protein environment has important implications to the understanding of the hydrophobic effects and their role in protein folding. Numerous parameters were developed previously to determine hydrophobicity of amino acid residues. However, these hydrophobicity scales are not always correlated consistently. Here, we constructed artificial planar peptide networks composed of unified amino acid side chains, considering both the primary and β-sheet secondary structure of the protein. Using molecular dynamics simulation, we computed the contact angle of a water nanodroplet on the peptide networks for all 20 types of amino acids. Our simulations offer a bridge that can connect thermodynamic hydrophobic data of amino acid residues and contact angle measurement widely used in engineering fields.

Author contributions: C.Z., Y.G., H.L., J.S.F., and X.C.Z. designed research; C.Z., Y.G., H.L., L.L., J.S.F., and X.C.Z. performed research; J.S.F. and X.C.Z. contributed new reagents/analytic tools; C.Z., Y.G., H.L., S.M., L.L., and X.C.Z. analyzed data; and C.Z., H.L., J.S.F., and X.C.Z. wrote the paper.

Reviewers: L.D., Pacific Northwest National Laboratory; and W.Y., Florida State University.

The authors declare no conflict of interest.

[1]C.Z., Y.G., and H.L. contributed equally to this work.

[2]To whom correspondence may be addressed. Email: jfrancisco3@unl.edu or xzeng1@unl.edu.

This article contains supporting information online at www.pnas.org/lookup/suppl/doi:10.1073/pnas.1616138113/-/DCSupplemental.

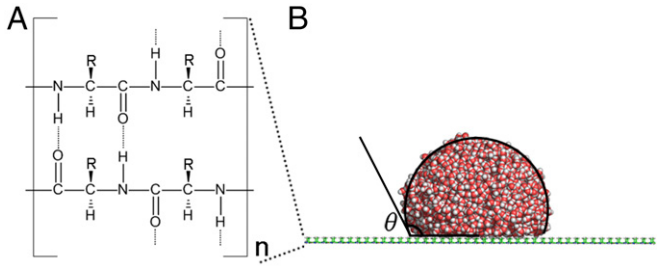

Fig. 1. (*A*) A schematic structure of artificial β-folding 2D peptide network composed of unified R-side chains, constructed considering both the primary and secondary structure of protein. (*B*) A side view of the MD simulation system and the definition of CA θ of a water nanodroplet.

typically entails hydrogen-bonding and dispersive interactions. Furthermore, the parameters attained from the partitioning method exhibit strong dependence on specific interactions among amino acids (or their derivatives), as well as the organic solvents used.

Note also that hydrophobicity of proteins can be characterized by computing accessible and buried surface areas of amino acids in known protein structures using statistical mechanics methods (44–48). However, the parameters obtained from the partitioning and statistical mechanics methods tend to be loosely correlated and may not be easily transferable from system to system. In some cases, the numerical values obtained for characterization of the hydrophobicity of certain amino acids are controversial. For example, the side chain of tyrosine has been identified as hydrophobic in some studies (18, 20, 21, 25) but hydrophilic in others (28, 29). Similar inconsistency was also seen for tryptophane (18, 20, 23, 25–27, 30, 31). Many studies only considered hydrophobicity of side chain analogs without considering conformation of the peptide backbone, which can also affect degrees of hydrophobicity of protein surface. Besides the primary structure, the secondary structure of proteins can also influence the hydrophobicity. For instance, Gromiha and Selvaraj (49) used hydrophobic characteristics to predict the secondary structures of proteins.

Atomistic molecular dynamics (MD) simulation has also been used to characterize hydrophobicity of protein, for which both side chain of amino acid residues and local configuration of peptide are considered. Important results on microscopic description of hydrophobicity of nanoscale surfaces have been obtained. For example, Garde and coworkers (39) computed density fluctuation of water at protein surface region to map out local hydrophobicity. Hajari and van der Vegt (16) computed molecular conditional solvation free energies to determine hydrophobicity of amino acid residues. These characterizations of hydrophobicity on the microscopic scales bring important insights into hydrophobic interaction and hydrophobic hydration but are not tightly correlated with the CA measurement that is widely used to characterize degrees of hydrophobicity (or wettability) of surfaces in engineering fields.

An important question is whether one can build a bridge that connects the hydrophobicity of amino acids in a protein environment and the CA measurement of surface wettability. To address the question, we developed an artificial planar surface of proteins to be in contact with a water nanodroplet. Note that a natural planar structure of protein is one of its secondary structures, namely, the β-pleated sheet, consisting of peptide strands connected laterally by backbone hydrogen bonds between N–H groups and C=O groups of adjacent strands, which generally forms a twisted and pleated sheet. The tiny twisted fragment of the β-sheet in natural protein is unfeasible for the CA measurement using the conventional method; however, it suggests to us another way to build a planar surface with the secondary structure of protein. Indeed, several recent experiments have shown evidence of 2D crystal of self-assembled protein-like peptoid polymers, held by electrostatics and dispersive interactions (50–54). Such a 2D protein-like sheet can mimic both the structure and functionality of protein, as well as provide a large-area planar surface for the CA measurement.

Following the secondary structures of proteins, particularly the patterns of hydrogen bonds between the main-chain peptide groups, we build 2D analogous networks with planar surface of specific amino acid side chains. We then use MD simulations to compute values of CA to characterize the hydrophobicity of amino acid side chains, with incorporating effects of both primary and secondary structures of protein backbones (see *Methods*). As another thermodynamic measure of the hydrophobicity and superhydrophilicity of the network surfaces, the excess chemical potential of a purely repulsive methane-sized Weeks–Chandler–Andersen (WCA) solute for all of the 20 types of amino acids is computed (55). With the computational data, we propose another hydrophobicity scale, for various amino acids in protein environment, that can be related to the CA measurement for characterizing wettability of surfaces.

Results and Discussion

Two-Dimensional Planar Peptide Networks. Both the primary and secondary structures are taken into account to construct the artificial 2D planar peptide networks. First, a polypeptide chain is built by conjoining amino acids of the same type, where amino acids are linked by peptide bonds. Next, based on the secondary structure of protein, the artificial polypeptide chains are linked together via hydrogen bonds, forming a 2D network. Meanwhile, all of the R-side chains of amino acids are uniformly located on one side of the surface of the artificial 2D network, as shown in Fig. 1*A*.

Considering that there are two types of β-folding peptides, namely, parallel and antiparallel β-sheets, in which the adjacent peptide chains are packed along the same or opposite orientation, we build both types of 2D networks for the MD simulations. The optimized structures of parallel and antiparallel 2D peptide networks with the Ala side chains are displayed in Fig. 2 *A*–*C* and *D*–*F*, respectively. As shown in Fig. 2, under the periodic boundary condition, both parallel and antiparallel 2D peptide networks exhibit atomically flat surface in the supercell, suggesting that the CA of a water droplet can be measured and analyzed on basis of Young's equation. Note that the N–H•••O hydrogen bonds in the antiparallel network are closer to linear configuration, indicating that the antiparallel β-sheets are energetically more stable than the parallel counterparts. With the Ala side chain, both network structures give nearly the same CA (θ = 118° for antiparallel β-sheets, and θ = 119° for parallel β-sheets) in the MD simulations (Fig. S1). Therefore, hereafter, we only focus on the hydrophobicity of antiparallel β-folding networks.

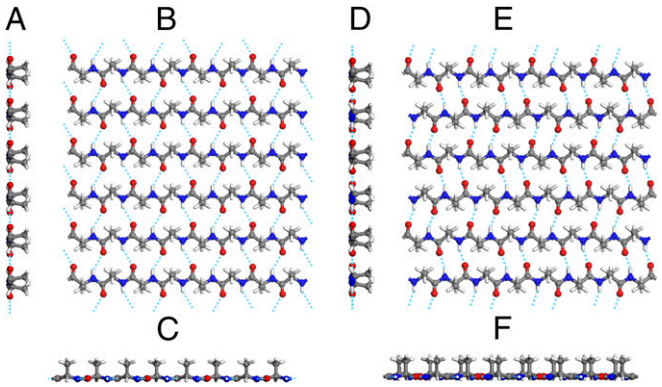

Fig. 2. Two side views and a top view of 2D peptide network, constructed by (*A*–*C*) parallel or (*D*–*F*) antiparallel β-sheet with the Alanine side chains along *x* (*A* and *D*), *z* (*B* and *E*), and *y* (*C* and *F*) direction. Both network structures are optimized using the DFT method.

Table 1. Computed density of R group in optimized 2D peptide network, each constructed by one of 20 types of amino acids

Acid type	Amino acid	Density, nm^{-2}
Nonpolar	Ile	4.83
	Ala	5.77
	Phe	4.96
	Leu	5.11
	Met	5.63
	Pro	4.80
	Val	4.95
	Trp	4.67
Polar	Cys	5.79
	Gly	5.88
	Thr	4.37
	Ser	5.72
	Tyr	5.02
	Gln	5.58
	Asn	5.88
Charged	His	5.35
	Lys	5.49
	Glu	5.49
	Arg	5.36
	Asp	5.73

Note also that the angles of N–H•••O hydrogen bonds in the antiparallel β-folding network are slightly titled to 160°, rather than the strictly linear structure, due to the dispersive interactions between adjacent peptide chains.

Likewise, the 2D peptide networks of the other 19 types of amino acids are optimized using density-functional theory (DFT) methods (Figs. S2–S4). Table 1 lists the density of R group in the 2D peptide networks. The densities of the 20 types of R groups follow the sequence Thr < Trp < Pro < Ile < Val < Phe < Tyr < Leu < His < Arg < Glu < Lys < Gln < Met < Ser < Asp < Ala < Cys < Gly < Asn, which is strongly dependent on the R-group size. Nevertheless, the difference in the R-group density among the 20 types of peptide networks is merely ∼7%. Such small differences are attributed to the strong N–H•••O hydrogen bonds and covalent peptide bonds, implying that the hydrophobicity of the 20 peptide networks is due mainly to the chemical properties of the amino acid residue.

CA Measurement. Based on the shape of an equilibrated sessile water nanodroplet on the 2D peptide networks from MD simulations, the CA (θ), defined as the averaged angle between the surface of the network and the tangential line of the nanodroplet [originated from the droplet–network interface (Fig. 1*B*)], is computed using a similar method to that reported previously (56). More specifically, the isochore line is traced as the liquid–vapor interface, at which the time-average density is half of the bulk density of water. Next, the CA can be measured by fitting the isochore line to a circle. As listed in Table 2, we compute CAs of water nanodroplets on various β-sheet networks where the corresponding amino acid side chains are divided into three groups: (*i*) nonpolar (Ile, Ala, Phe, Leu, Met, Pro, Val, Trp), (*ii*) polar (Cys, Gly, Thr, Ser, Tyr, Gln, Asn), and (*iii*) charged (His, Lys, Glu, Arg, Asp) side chains.

Snapshots of the water nanodroplet on antiparallel β-sheets with nonpolar amino acid side chains are shown in Fig. 3*A*. For better visualization, one of 20 MD trajectories for the water nanodroplet on a peptide network surface at 300 K is shown in Movie S1. Here, the 2D peptide networks with the nonpolar amino acid side chains exhibit hydrophobic behavior [$\theta > 90°$ (Table 2)]. The difference in θ among the nonpolar amino acid side chains is very small ($\Delta\theta < 16°$). In particular, CAs of the water nanodroplet on the β-sheets with Pro, Leu, Met, Pro, Val, or Trp side chains are nearly the same, i.e., $\theta \approx 110°$.

The CAs of water nanodroplets on peptide networks with polar amino acid side chains, i.e., Cys, Gly, Thr, Ser, Tyr, Gln, or Asn, are shown in Fig. 3*B* and Table 2. All networks with polar amino acid side chains exhibit hydrophilicity ($\theta < 90°$). Moreover, the CAs show big differences, with $\Delta\theta$ ranging from 0° to 85.4°. Because the peptide networks with Tyr, Gln, or Asn side chains exhibit complete-wetting behavior ($\theta = 0$), these networks can be viewed as superhydrophilic. In cases of amino acids possessing ionic groups on side chains, sodium or chloride ions can be added to neutralize the system. All of the Lennard-Jones parameters and atomic net charges are still taken from Amber force field. All peptide networks with the charged amino acid side chains show complete-wetting behavior ($\theta = 0°$).

Excess Chemical Potentials. For the network surfaces with $\theta = 0$, measurement of the hydrophobicity requires a different scale. We also computed the excess chemical potentials ($\Delta\mu^{ex}_{bulk}$) of the purely repulsive methane-sized WCA solute ($\sigma = 0.345$ nm, $\varepsilon = 0.896$ kJ/mol), with respect to that in the bulk (Figs. S5 and S6), as an alternative thermodynamic indicator of hydrophobicity. A minimum value in $\Delta\mu^{ex}_{bulk}$ is clearly observed near the surface for all nonpolar amino acid side chains (Fig. S5). We move all of the curves such that their minimums are all located at $z^* = 0$. The depths of the minimum $\Delta\mu^{ex}_{int}$ for the eight nonpolar amino acid side chains are shown in Table 2.

Previous studies show that formation of a cavity is more favorable near the solute/water interface than in the bulk (57–59). Because of its relation with the cavity formation probability, the excess chemical potential of a hard-sphere solute can be used as a microscopic measure of the hydrophobicity of the solute–water interface (38, 39). Our MD simulation indicates that the methane-sized WCA solute's chemical potential in bulk water, μ^{ex}_{bulk}, is about 32.2 kJ/mol. Figs. S5 and S6 show the excess chemical potential of the methane-sized WCA solute along the direction normal to the β-sheet network, with respect to that in the bulk, where a minimum is seen at

Table 2. Computed CAs of a water nanodroplet on the artificial β-sheets with various amino acid side chains, and excess chemical potential of purely repulsive WCA solutes at the 2D peptide network–nanodroplet interfaces with respect to their chemical potential in bulk water

Acid type	Amino acids	θ, deg	cos θ	$\Delta\mu^{ex}_{int}$, kJ/mol
Nonpolar	Ile	121.8 ± 0.3	−0.528	−9.73
	Ala	119.7 ± 0.7	−0.495	−9.58
	Phe	111.7 ± 0.6	−0.370	−9.23
	Leu	110.0 ± 0.4	−0.342	−8.66
	Met	108.9 ± 0.3	−0.324	−7.65
	Pro	108.8 ± 0.5	−0.322	−7.55
	Val	107.9 ± 0.2	−0.308	−8.26
	Trp	105.7 ± 0.6	−0.270	−8.62
Polar	Cys	85.4 ± 0.1	0.081	−5.63
	Gly	67.3 ± 0.5	0.386	−4.57
	Thr	31.5 ± 2.3	0.853	−4.06
	Ser	20.6 ± 1.7	0.936	−3.56
	Tyr	∼0	1.677*	−0.05
	Gln	∼0	2.176*	2.02
	Asn	∼0	2.354*	2.76
Charged	His	∼0	2.029*	1.41
	Lys	∼0	2.101*	1.71
	Glu	∼0	3.173*	6.16
	Arg	∼0	4.383*	11.18
	Asp	∼0	9.573*	32.72

*Cosine values of the CA are calculated based on Eq. **1**.

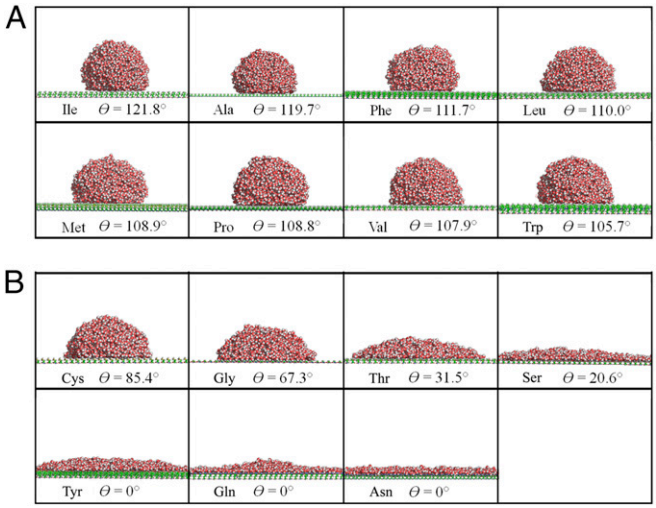

Fig. 3. Snapshots of a water nanodroplet on antiparallel β-sheet (*A*) with nonpolar amino acid side chains or (*B*) with polar amino acid side chains, near the end of MD simulation.

the network–water interface for nonpolar amino acid side chains. Fig. 4 shows the excess chemical potential of the probe solute at the network–water interface, defined by the depth of the minimum, $\Delta\mu_{int}^{ex}$, as a function of cos θ. According to previous studies, $\Delta\mu_{int}^{ex}$ exhibits a linear dependence on cos θ (38, 39). The solid line in Fig. 4 represents a linear fit to all data points (with $\theta > 0$) using the least square algorithm. The fitted straight line can be given by

$$\Delta\mu_{int}^{ex} = 4.15\cos\theta - 7.01. \quad [1]$$

To quantify the hydrophobicity of amino acid side chains with $\theta = 0$, the extrapolated values of cos θ are calculated according to Eq. **1** with $\Delta\mu_{int}^{ex}$ being the input (see * in Table 2). For the three polar amino acid side chains with $\theta = 0$, we found that the hydrophobicity decreases in the sequence of Tyr < Gln < Asn. For the five charged amino acid side chains with $\theta = 0$, the hydrophilicity decreases in the sequence of His < Lys < Glu < Arg < Asp. It is worth mentioning that the excess chemical potential shows greater difference for charged amino acid side chains than for polar amino acid side chains, ranging from 1.41 kJ/mol to 32.72 kJ/mol. Also, only His and Lys are apparently more hydrophobic than the two most hydrophilic polar amino acids, Gln and Asn (Table 2).

Comparison with Other Hydrophobicity Scales. To validate the computational measurement of wettability of amino acid side chains on the basis of the artificial planar peptide networks, we compare the hydrophobicity data obtained from our simulations to previously reported hydrophobicity scales of amino acid residues, which include the experimental free energies of transfer relative to glycine (13) (Fig. 5*A*), computed free energies based on accessible surface areas (30) (Fig. 5*B*), conditional solvation free energies based on empirical force-field model (18) (Fig. 5*C*), and calculated hydrophobic moments based on solvation energies (29) (Fig. 5*D*). For the hydrophilic amino acids ($\theta < 90°$), we found that the previously reported hydrophobicity scales show more or less linear correlation with cos θ values obtained from our simulations, including the experimental free energies of transfer (Fig. 5*A*).

However, such a similarity in trends becomes nonapparent for nonpolar side chains (black squares in Fig. 5) due largely to small hydration energy for nonpolar side chains. From our simulations, all of the eight nonpolar side chains show hydrophobic behavior ($\theta > 90°$; Table 2). Specifically, the difference in θ among the nonpolar amino acid side chains is small ($\Delta\theta < 16°$). In particular, the θ values for Val, Leu, Met, Pro, and Trp side chains are almost the same (about 110°). Hence, our simulations suggest that the amino acid residues with nonpolar side chains entail nearly the same hydrophobicity. Note that certain inconsistencies between surface accessibility of each amino acid and its hydrophobicity have also been reported previously (60). For example, no linear correlation between the conditional solvation free energy and the buried area of individual side chains upon folding for nonpolar amino acids is seen (18).

Conclusion

In conclusion, based on the structures of β-sheet, artificial 2D planar peptide networks are constructed with the unified amino acid side chains. Using MD simulations, we examined the hydrophobicity of 20 types of amino acids by measuring the CA of a water nanodroplet on the corresponding planar peptide networks. Our simulations show that all nonpolar amino acid side chains are hydrophobic ($\theta > 90°$), even though their peptide backbones are highly charged. The difference in θ among the nonpolar amino acid side chains is very small. For the polar amino acid side chains, the θ values show bigger differences. For the charged amino acid side chains, their peptide networks display complete-wetting behavior ($\theta = 0°$). To further characterize the hydrophobicity of the polar and charged amino acid side chains that display complete-wetting behavior, excess chemical potential of purely repulsive WCA solute at the network–water interface, with respect to the chemical potential in bulk water, $\Delta\mu_{int}^{ex}$, is computed. Based on a linear fit between $\Delta\mu_{int}^{ex}$ and cos θ, artificial cosθ values are obtained to characterize the hydrophobicity of polar and charged amino acid side chains. These numerical results offer a different hydrophobicity scale for various amino acids in protein environment, which can be also related to the CA measurement for characterizing wettability of surfaces. Our simulations offer a bridge connecting thermodynamic hydrophobic data of amino acid residues and macroscopic wettability measurement used in chemical engineering fields.

Methods

Unit Cell Structure of 2D Protein. The unit cell structure of 2D planar peptide networks is optimized using the first-principle method within the framework

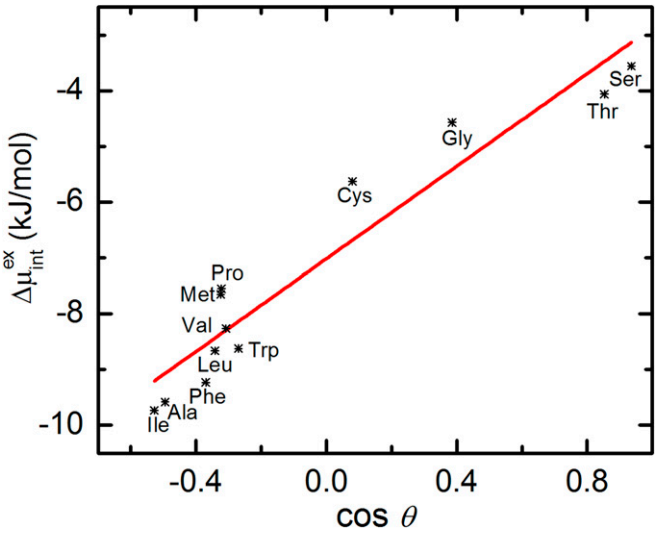

Fig. 4. Excess chemical potential of purely repulsive WCA solute at the network–water interface, with respect to the corresponding chemical potential in bulk water ($\Delta\mu_{int}^{ex}$), versus the cosine value of the CA (cos θ).

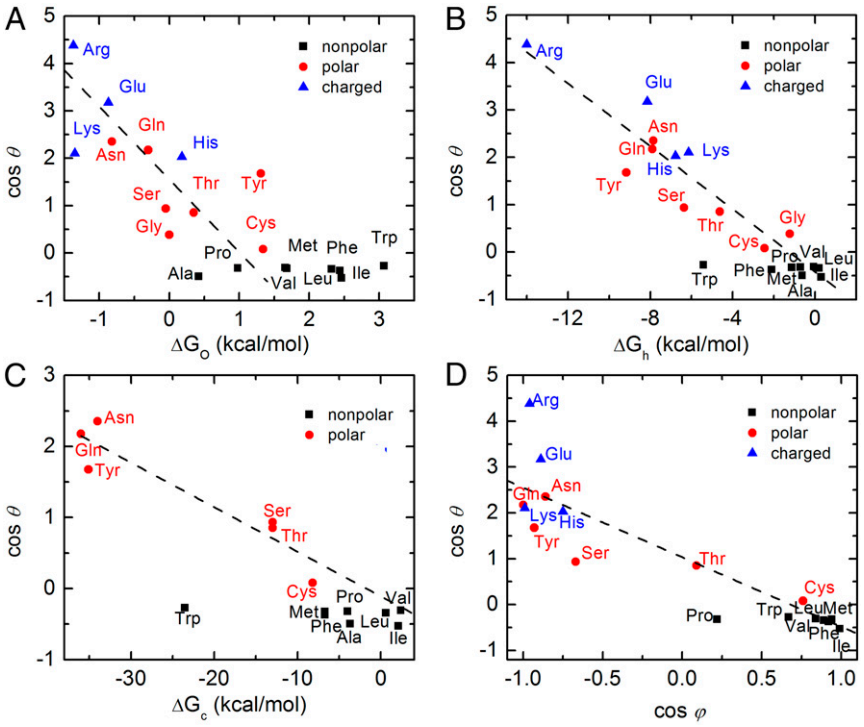

Fig. 5. Correlation between cos θ values obtained from our simulations and several hydrophobicity scales obtained from previous studies: (*A*) The experimental free energies of transfer relative to glycine, (*B*) computed free energies based on accessible surface areas, (*C*) conditional solvation free energies based on empirical force field model, and (*D*) calculated hydrophobic moments based on solvation energies for different polar amino acid side chains. The black squares, red circles, and blue triangles correspond to the nonpolar, polar, and charged amino acids, respectively.

of DFT implemented in Vienna Ab initio Simulation Package (61). The generalized gradient approximation in the form of Perdew–Burke–Ernzerh is used, combined with the projector-augmented wave pseudopotential and the plane–wave basis set with a cutoff energy of 500 eV. The intermolecular dispersion interaction is taken into account by choosing a van der Waals density functional method (62). A sufficiently large vacuum space (> 15 Å) in the surface normal (*z*) direction is adopted so that the interaction between the periodic images can be neglected. The Brillouin zone is sampled with a $3 \times 3 \times 1$ Monkhorst–Pack k mesh. During the geometry optimization, the carbon atoms in the backbone are fixed in the surface normal (*z*) direction while other atoms are allowed to relax in all directions until the force on each atom is less than 10^{-4} eV/Å, to ensure accurate convergence.

CA Measurement. After geometric optimization, a cuboid box of 3,009 water molecules is placed 3 Å above the surface of the 2D peptide network containing 34 polypeptide chains, each having 43 amino acids. A supercell ($20.0 \times 20.0 \times 20.0$ nm^3) with the periodic boundary conditions along in-plane directions (*x* and *y* directions) is selected for the systems. Again, to keep the planar surface of the 2D peptide network, the carbon and nitrogen atoms in backbone are fixed while other atoms are allowed to relax during the MD simulations. The rigid extended simple point charge potential model (63) is selected for water, and the Amber force fields are used for amino acids. The electrostatic interactions are computed using the particle mesh Ewald algorithm (64). The leapfrog Verlet integration algorithm is applied. All MD simulations are performed, using the Gromacs 4.4.5 package (65), in the canonical ensemble with the temperature controlled at 300 K. The MD simulation time is 7 ns (with a time step of 2 fs) for each peptide network. Data collected in the final 1 ns are used for analysis (66–70).

Excess Chemical Potential. For these simulations, each planar peptide network (Fig. S7) includes eight polypeptide chains, each having 12 amino acids, and the periodic boundary conditions are applied along the in-plane directions (*x* and *y* directions); 1,599 water molecules are included in the periodic box. The excess chemical potential of a methane-sized WCA solute (with the size parameter of $\sigma = 0.373$ nm) is computed using the Widom particle insertion method (71–73).

ACKNOWLEDGMENTS. We thank Professor Wenchuan Wang at Beijing University of Chemical Technology for valuable discussions. This work is supported by the National Science Foundation (CHE-1500217 and CBET-1512164) and National Natural Science Foundation of China (11374333), by a fund from Beijing Advanced Innovation Center for Soft Matter Science & Engineering for summer visiting scholar, and by the University of Nebraska Holland Computing Center.

1. Engelman DM, Steitz TA, Goldman A (1986) Identifying nonpolar transbilayer helices in amino acid sequences of membrane proteins. *Annu Rev Biophys Biophys Chem* 15: 321–353.
2. Kauzmann W (1959) Some factors in the interpretation of protein denaturation. *Adv Protein Chem* 14:1–63.
3. Tanford C (1978) The hydrophobic effect and the organization of living matter. *Science* 200(4345):1012–1018.
4. Dill KA (1990) Dominant forces in protein folding. *Biochemistry* 29(31):7133–7155.
5. Dill KA, MacCallum JL (2012) The protein-folding problem, 50 years on. *Science* 338(6110):1042–1046.
6. Dill KA (1990) The meaning of hydrophobicity. *Science* 250(4978):297–298.
7. Honig B, Yang AS (1995) Free energy balance in protein folding. *Adv Protein Chem* 46(46):27–58.
8. Nozaki Y, Tanford C (1971) The solubility of amino acids and two glycine peptides in aqueous ethanol and dioxane solutions. Establishment of a hydrophobicity scale. *J Biol Chem* 246(7):2211–2217.
9. Yunger LM, Cramer RD, 3rd (1981) Measurement of correlation of partition coefficients of polar amino acids. *Mol Pharmacol* 20(3):602–608.
10. Lawson EQ, et al. (1984) A simple experimental model for hydrophobic interactions in proteins. *J Biol Chem* 259(5):2910–2912.
11. Damodaran S, Song KB (1986) The role of solvent polarity in the free energy of transfer of amino acid side chains from water to organic solvents. *J Biol Chem* 261(16):7220–7222.
12. Fauchere JL, Pliska V (1983) Hydrophobic parameters Π of amino-acid side-chains from the partitioning of N-acetyl-amino-acid amides. *Eur J Med Chem* 18(4): 369–375.
13. Radzicka A, Wolfenden R (1988) Comparing the polarities of the amino-acids: Side-chain distribution coefficients between the vapor phase, cyclohexane, 1-octanol, and neutral aqueous solution. *Biochemistry-Us* 27(5):1664–1670.
14. Palecz B (2002) Enthalpic homogeneous pair interaction coefficients of L-alpha-amino acids as a hydrophobicity parameter of amino acid side chains. *J Am Chem Soc* 124(21):6003–6008.

15. Palecz B (2005) Enthalpic pair interaction coefficient between zwitterions of L-alpha-amino acids and urea molecule as a hydrophobicity parameter of amino acid side chains. *J Am Chem Soc* 127(50):17768–17771.
16. Hajari T, van der Vegt NFA (2014) Peptide backbone effect on hydration free energies of amino acid side chains. *J Phys Chem B* 118(46):13162–13168.
17. Cornette JL, et al. (1987) Hydrophobicity scales and computational techniques for detecting amphipathic structures in proteins. *J Mol Biol* 195(3):659–685.
18. Levitt M (1976) A simplified representation of protein conformations for rapid simulation of protein folding. *J Mol Biol* 104(1):59–107.
19. Janin J (1979) Surface and inside volumes in globular proteins. *Nature* 277(5696): 491–492.
20. Hopp TP, Woods KR (1981) Prediction of protein antigenic determinants from amino acid sequences. *Proc Natl Acad Sci USA* 78(6):3824–3828.
21. Sweet RM, Eisenberg D (1983) Correlation of sequence hydrophobicities measures similarity in three-dimensional protein structure. *J Mol Biol* 171(4):479–488.
22. Matsumura M, Becktel WJ, Matthews BW (1988) Hydrophobic stabilization in T4 lysozyme determined directly by multiple substitutions of Ile 3. *Nature* 334(6181): 406–410.
23. Fauchère JL, Charton M, Kier LB, Verloop A, Pliska V (1988) Amino acid side chain parameters for correlation studies in biology and pharmacology. *Int J Pept Protein Res* 32(4):269–278.
24. Miyazawa S, Jernigan RL (1985) Estimation of effective interresidue contact energies from protein crystal structures: Quasi-chemical approximation. *Macromolecules* 18(3): 534–552.
25. Kidera A, Konishi Y, Oka M, Ooi T, Scheraga HA (1985) Statistical analysis of the physical properties of the 20 naturally occurring amino acids. *J Protein Chem* 4(1):23–55.
26. Parker JMR, Guo D, Hodges RS (1986) New hydrophilicity scale derived from high-performance liquid chromatography peptide retention data: Correlation of predicted surface residues with antigenicity and X-ray-derived accessible sites. *Biochemistry* 25(19):5425–5432.
27. Eisenberg D, McLachlan AD (1986) Solvation energy in protein folding and binding. *Nature* 319(6050):199–203.
28. Ooi T, Oobatake M, Némethy G, Scheraga HA (1987) Accessible surface areas as a measure of the thermodynamic parameters of hydration of peptides. *Proc Natl Acad Sci USA* 84(10):3086–3090.
29. Oobatake M, Ooi T (1988) Characteristic thermodynamic properties of hydrated water for 20 amino acid residues in globular proteins. *J Biochem* 104(3):433–439.
30. Chmelik J, et al. (1991) Characterization of the hydrophobic properties of amino acids on the basis of their partition and distribution coefficients in the 1-octanol-water system. *Collect Czech Chem Commun* 56(10):2030–2041.
31. Norinder U (1991) Theoretical amino acid descriptors. Application to bradykinin potentiating peptides. *Peptides* 12(6):1223–1227.
32. van de Waterbeemd H, Karajiannis H, El Tayar N (1994) Lipophilicity of amino acids. *Amino Acids* 7(2):129–145.
33. Yoshida T (1998) Calculation of peptide retention coefficients in normal-phase liquid chromatography. *J Chromatogr A* 808(1-2):105–112.
34. Chang J, Lenhoff AM, Sandler SI (2007) Solvation free energy of amino acids and side-chain analogues. *J Phys Chem B* 111(8):2098–2106.
35. König G, Bruckner S, Boresch S (2013) Absolute hydration free energies of blocked amino acids: Implications for protein solvation and stability. *Biophys J* 104(2):453–462.
36. König G, Boresch S (2009) Hydration free energies of amino acids: Why side chain analog data are not enough. *J Phys Chem B* 113(26):8967–8974.
37. Biswas KM, DeVido DR, Dorsey JG (2003) Evaluation of methods for measuring amino acid hydrophobicities and interactions. *J Chromatogr A* 1000(1-2):637–655.
38. Godawat R, Jamadagni SN, Garde S (2009) Characterizing hydrophobicity of interfaces by using cavity formation, solute binding, and water correlations. *Proc Natl Acad Sci USA* 106(36):15119–15124.
39. Jamadagni SN, Godawat R, Garde S (2011) Hydrophobicity of proteins and interfaces: Insights from density fluctuations. *Annu Rev Chem Biomol Eng* 2:147–171.
40. Granick S, Bae SC (2008) Chemistry. A curious antipathy for water. *Science* 322(5907): 1477–1478.
41. Fendler JH, Nome F, Nagyvary J (1975) Compartmentalization of amino acids in surfactant aggregates. Partitioning between water and aqueous micellar sodium deodecanoate and between hexane and dodecylammonium propionate trapped water in hexane. *J Mol Evol* 6(3):215–232.
42. Leodidis EB, Hatton TA (1990) Amino-acids in AOT reversed micelles. 1. Determination of interfacial partition coefficients using the phase-transfer method. *J Phys Chem* 94(16):6400–6411.
43. Baldwin RL (2013) The new view of hydrophobic free energy. *FEBS Lett* 587(8): 1062–1066.
44. Chothia C (1976) The nature of the accessible and buried surfaces in proteins. *J Mol Biol* 105(1):1–12.
45. Lee B, Richards FM (1971) The interpretation of protein structures: Estimation of static accessibility. *J Mol Biol* 55(3):379–400.
46. Meirovitch H, Rackovsky S, Scheraga HA (1980) Empirical studies of hydrophobicity. 1. Effect of protein size on the hydrophobic behavior of amino acids. *Macromolecules* 13(6):1398–1405.
47. Manavalan P, Ponnuswamy PK (1978) Hydrophobic character of amino acid residues in globular proteins. *Nature* 275(5681):673–674.
48. Janin J (2008) Biochemistry. Dicey assemblies. *Science* 319(5860):165–166.
49. Gromiha MM, Selvaraj S (1998) Protein secondary structure prediction in different structural classes. *Protein Eng* 11(4):249–251.
50. Nam KT, et al. (2010) Free-floating ultrathin two-dimensional crystals from sequence-specific peptoid polymers. *Nat Mater* 9(5):454–460.
51. Kudirka R, et al. (2011) Folding of a single-chain, information-rich polypeptoid sequence into a highly ordered nanosheet. *Biopolymers* 96(5):586–595.
52. Sanii B, et al. (2011) Shaken, not stirred: Collapsing a peptoid monolayer to produce free-floating, stable nanosheets. *J Am Chem Soc* 133(51):20808–20815.
53. Olivier GK, et al. (2013) Antibody-mimetic peptoid nanosheets for molecular recognition. *ACS Nano* 7(10):9276–9286.
54. Tran H, Gael SL, Connolly MD, Zuckermann RN (2011) Solid-phase submonomer synthesis of peptoid polymers and their self-assembly into highly-ordered nanosheets. *J Vis Exp* 57:e3373.
55. Weeks JD, Chandler D, Andersen HC (1971) Role of repulsive forces in determining equilibrium structure of simple liquids. *J Chem Phys* 54(12):5237.
56. Zhu C, Li H, Huang Y, Zeng XC, Meng S (2013) Microscopic insight into surface wetting: Relations between interfacial water structure and the underlying lattice constant. *Phys Rev Lett* 110(12):126101.
57. Willard AP, Chandler D (2008) The role of solvent fluctuations in hydrophobic assembly. *J Phys Chem B* 112(19):6187–6192.
58. Jamadagni SN, Godawat R, Garde S (2009) How surface wettability affects the binding, folding, and dynamics of hydrophobic polymers at interfaces. *Langmuir* 25(22):13092–13099.
59. Patel AJ, Varilly P, Chandler D (2010) Fluctuations of water near extended hydrophobic and hydrophilic surfaces. *J Phys Chem B* 114(4):1632–1637.
60. Moelbert S, Emberly E, Tang C (2004) Correlation between sequence hydrophobicity and surface-exposure pattern of database proteins. *Protein Sci* 13(3):752–762.
61. Kresse G, Furthmüller J (1996) Efficient iterative schemes for ab initio total-energy calculations using a plane-wave basis set. *Phys Rev B Condens Matter* 54(16):11169–11186.
62. Klimeš J, Bowler DR, Michaelides A (2010) Chemical accuracy for the van der Waals density functional. *J Phys Condens Matter* 22(2):022201.
63. Berendsen HJC, Grigera JR, Straatsma TP (1987) The missing term in effective pair potentials. *J Phys Chem* 91(24):6269–6271.
64. Essmann U, et al. (1995) A smooth particle mesh Ewald method. *J Chem Phys* 103(19): 8577–8593.
65. Lindahl E, Hess B, van der Spoel D (2001) GROMACS 3.0: A package for molecular simulation and trajectory analysis. *J Mol Model* 7(8):306–317.
66. Hautman J, Klein ML (1991) Microscopic wetting phenomena. *Phys Rev Lett* 67(13): 1763.
67. Koishi T, Yasuoka K, Fujikawa S, Ebisuzaki T, Zeng XC (2009) Coexistence and transition between Cassie and Wenzel state on pillared hydrophobic surface. *Proc Natl Acad Sci USA* 106(21):8435–8440.
68. Li H, Zeng XC (2012) Wetting and interfacial properties of water nanodroplets in contact with graphene and monolayer boron-nitride sheets. *ACS Nano* 6(3): 2401–2409.
69. Koishi T, Yasuoka K, Fujikawa S, Zeng XC (2011) Measurement of contact-angle hysteresis for droplets on nanopillared surface and in the Cassie and Wenzel states: A molecular dynamics simulation study. *ACS Nano* 5(9):6834–6842.
70. Koishi T, Yasuoka K, Zeng XC, Fujikawa S (2010) Molecular dynamics simulations of urea-water binary droplets on flat and pillared hydrophobic surfaces. *Faraday Discuss* 146:185–193.
71. Widom B (1963) Some topics in theory of fluids. *J Chem Phys* 39(11):2808–2812.
72. Widom B (1982) Potential distribution theory and the statistical mechanics of fluids. *J Phys Chem* 86(6):869–872.
73. Pohorille A, Pratt LR (1990) Cavities in molecular liquids and the theory of hydrophobic solubilities. *J Am Chem Soc* 112(13):5066–5074.